

Uncertainty-aware Gait Recognition via Learning from Dirichlet Distribution-based Evidence

Beibei Lin*, Chen Liu*, Ming Wang, Lincheng Li, Shunli Zhang, Robby T. Tan, and Xin Yu†

Abstract—Existing gait recognition frameworks retrieve an identity in the gallery based on the distance between a probe sample and the identities in the gallery. However, existing methods often neglect that the gallery may not contain identities corresponding to the probes, leading to recognition errors rather than raising an alarm. In this paper, we introduce a novel uncertainty-aware gait recognition method that models the uncertainty of identification based on learned evidence. Specifically, we treat our recognition model as an evidence collector to gather evidence from input samples and parameterize a Dirichlet distribution over the evidence. The Dirichlet distribution essentially represents the density of the probability assigned to the input samples. We utilize the distribution to evaluate the resultant uncertainty of each probe sample and then determine whether a probe has a counterpart in the gallery or not. To the best of our knowledge, our method is the first attempt to tackle gait recognition with uncertainty modelling. Moreover, our uncertain modeling significantly improves the robustness against out-of-distribution (OOD) queries. Extensive experiments demonstrate that our method achieves state-of-the-art performance on datasets with OOD queries, and can also generalize well to other identity-retrieval tasks. Importantly, our method outperforms the state-of-the-art by a large margin of 51.26% when the OOD query rate is around 50% on OUMVLP.

Index Terms—Gait Recognition, Out-of-distribution

1 INTRODUCTION

Gait recognition, as an important biometric retrieval task, aims to identify people by their way of walking [1], and it is widely used in security monitoring and forensics. Gait recognition has been formulated as a retrieval task, where a query gait sequence, namely a probe, is compared to gait sequences from a gallery. The sequence from the gallery that has the minimal distance to the probe will be regarded as a match and finally its identity will be assigned to the probe.

Existing gait recognition methods assume there are always corresponding identities in the gallery set. However, in practice, this assumption often does not hold. Some probes possibly do not have their corresponding identities in the gallery, which we call out-of-distribution (OOD) queries. As shown in Fig.1(a), current methods still find an identity from the gallery even though actually there is no identity of the probe in the gallery, leading to erroneous results. Therefore, it is highly desirable to develop a gait recognition method that is able to not only find correct identities but also to identify OOD queries. Unfortunately, existing methods that often formulate gait recognition as a feature matching problem do not have a mechanism to address the OOD cases.

In contrast to existing gait recognition approaches, in this work, we formulate gait recognition as an uncertainty-aware feature matching problem. We propose an uncertainty-aware gait recognition framework that can effectively address both in-distribution and out-of-distribution queries. Our uncertainty-aware framework is agnostic against gait recognition networks, and thus

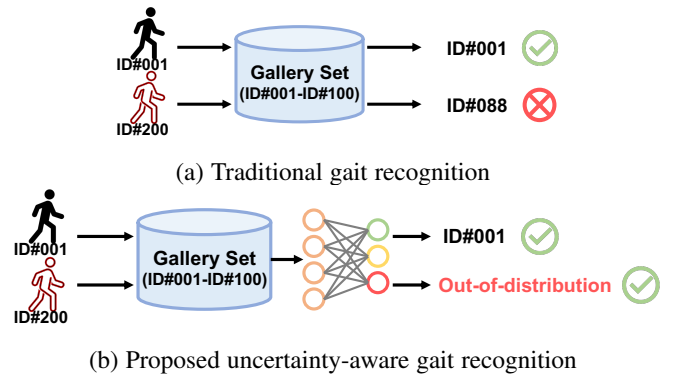


Fig. 1. The in-distribution and out-of-distribution cases for traditional gait recognition framework, and our uncertainty-aware gait recognition framework, which handles OOD queries.

it can adopt any existing gait recognition network as a feature extractor from a probe and gallery sequences. Once we obtain the features of gait sequences, we will retrieve the gallery feature that has the minimal distance to that of the probe. Unlike existing methods that directly assign the identity to the probe, we further determine whether the probe and gallery features are from the same identity or not, as shown in Fig.1(b).

To examine the identity matches between the probe and gallery, we introduce the theory of evidential deep learning into the process of feature matching. Evidential deep learning [2], [3], [4] regards deep networks as an evidence collector and models class probabilities via a Dirichlet distribution. Motivated by this, we propose a gait classification model that is employed as an evidence collector to gather opinions or evidence from the paired features of the probe and gallery. The evidence is then utilized to parameterize a Dirichlet distribution. Moreover, the theory of

- Beibei Lin and Robby T. Tan were with the National University of Singapore,
- Chen Liu and Xin Yu were with the University of Queensland, Australia.
- Lincheng Li was with the Fuxi Lab, NetEase, Hangzhou, China.
- Ming Wang and Shunli Zhang were with the School of Software Engineering, Beijing Jiaotong University, Beijing, China.
- * Joint first authors
- † Xin Yu is the corresponding author. E-mail: xin.yu@uq.edu.au

Subjective Logic [2] indicates that the Dirichlet distribution represents the probability density of the input features, including in-distribution and out-distribution query scenarios. In other words, the Dirichlet distribution reflects the mass assignment of the input features and their uncertainty in the feature space, thus providing a mechanism to detect OOD probes. Once we obtain the Dirichlet distribution parameterized over the input features, we can apply it to examine whether a pair of retrieved gaits is from the same person and how confident our prediction is. As a result, our model predicts three scores: a matching score, an unmatching score and an uncertainty score. Based on the three scores, we are able to determine in-distribution and out-of-distribution queries.

Extensive experiments demonstrate that our method achieves state-of-the-art performance on gait recognition with OOD queries. Importantly, our method outperforms the state-of-the-art method, *i.e.*, DyGait [5], by a large margin of 51.26% when the rate of OOD queries is 50% on one of the largest gait recognition datasets OUMVLP [6]. Our main contributions are summarized as follows:

- 1) We propose a novel uncertainty-aware gait recognition model that can tackle both in-distribution and out-of-distribution queries in a unified framework. To the best of our knowledge, we are the first to address OOD cases for gait recognition.
- 2) We introduce the theory of evidential deep learning to represent the probability density of a pair of retrieved features and thus model the uncertainty of our prediction.
- 3) Our framework is agnostic against gait recognition backbones. It can be adopted by existing methods with minimal effort to address OOD queries, thus significantly improving their robustness.

2 RELATED WORK

Gait Recognition Gait recognition aims to learn discriminative feature representations from people’s skeletons or silhouettes for identification purposes [7], [8], [9], [10], [11], [12], [13]. Its objective is to obtain the identity information for a probe sample from the gallery. To achieve this goal, many studies focus on improving the feature extraction capability of the model. These methods can be categorized into three classes, *i.e.*, model-based methods, pose-based methods, and silhouette-based methods. Model-based methods are designed to extract features from RGB sequences, such as shapes, view angles, and postures [14], [15], [16]. Pose-based methods extract 2D poses or 3D poses of human bodies to obtain discriminative feature representations [17], [18], [19], [20]. Silhouette-based methods generate feature representations by aggregating all temporal information of a gait sequence [21], [22], [23], [24], [25], [26], [27], [28], [29], [30], [31], [32], [33], [34], [35], [36], [37], [38], [39], [40]. Although the above methods obtain high recognition accuracy, they often neglect the fact that a probe might be an OOD sample, which does not have counterparts in the gallery. When such probes are exhibited, current methods would fail and cannot tell the gallery does not contain corresponding identities as they do not have a mechanism to address OOD queries. To the best of our knowledge, our work is the first attempt to address the OOD query scenario in gait recognition.

Moreover, many other recognition tasks, such as vehicle and human re-identification [41], [42], [43] and face recognition [44], [45], also follow a very similar recognition paradigm as gait recognition, and thus face the same situation of OOD queries.

Therefore, our method can be readily applied to those tasks to improve their recognition robustness against OOD queries, thus avoiding incorrect identity assignments. In addition, our method does not need to re-train the backbone networks, significantly facilitating existing networks to adapt to OOD queries.

OOD Recognition In our task, the test set involves identities that have been seen and unseen in the training set. If a testing identity is not registered to the gallery set but exists in the probe set, it will be regarded as an OOD identity. Open-set recognition methods [46], [47] have been proposed to address the OOD problem in recognition. These methods aim to classify the known classes while labeling all OOD samples to one unknown class. However, they cannot be used for our task. This is because query identities that have been unseen in the training set will be regarded as unknown classes by open-set recognition methods, while our method still needs to find their counterparts from the gallery set, and the query identities are usually not provided in training.

3 UNCERTAINTY-AWARE GAIT RECOGNITION FRAMEWORK

Existing gait recognition methods follow a standard paradigm, which can be divided into three steps: (i) Designing and training a gait recognition network. The gait recognition network can be trained with various losses to achieve strong feature extraction capability. (ii) Extracting features. Once the gait recognition network has been trained, we use it to extract features from a sequence sampled from the probe and gallery sets. Here, we denote $\mathbb{Q} = \{q_1, q_2, \dots, q_M\}$ as all the probe features from the probe set and $\mathbb{G} = \{g_1, g_2, \dots, g_N\}$ as all the gallery features from the gallery set, where q_i is i -th probe feature, g_j is the j -th gallery feature, and M and N indicate the number of the probe samples and gallery samples, respectively; (iii) Computing the distance to the gallery features. We compute the distance between a probe feature q_i and all the gallery features. For a probe feature q_i , its distances with respect to all the gallery features can be represented as $\mathbb{D}_i = \{D(q_i, g_1), D(q_i, g_2), \dots, D(q_i, g_N)\}$, where D indicates the Euclidean distance in our experiments. Subsequently, we find the minimum distance in \mathbb{D}_i . Suppose $D(q_i, g_j)$ is the minimum value in \mathbb{D}_i , and then the identity of g_j will be assigned to the probe i .

However, in step (iii), conventional gait recognition methods neglect the fact there might be no matching identity in the gallery. Although $D(q_i, g_j)$ is minimum, the identity j should not be assigned to the probe i . When the probe does not have a counterpart identity in the gallery, we refer to it as an OOD query. To address both in-distribution and out-of-distribution queries in a unified framework, we present an uncertainty-aware gait recognition method, as illustrated in Figure 2.

3.1 Dirichlet-based Evidence Learning

To address both in-distribution and out-of-distribution queries in a unified framework, our work aims to model the probability distribution of the distance of gait features and estimate the uncertainty of our classification model. Previous methods estimate prediction variance or uncertainty through dropout [48], [49], [50], [51], ensembling [52], [53] or other sampling approaches [54], [55]. However, this stream of works often relies on expensive sampling operations and it is hard to apply them to feature matching tasks, since the probe and gallery features are often fixed.

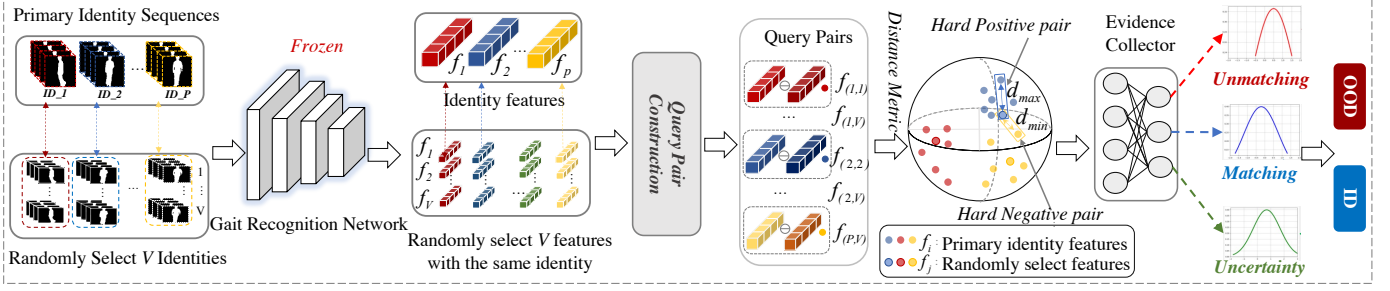


Fig. 2. Overview of the uncertainty-aware gait recognition framework. We first utilize existing backbones to extract features and then construct hard positive and negative feature pairs to train our evidence collector. By Dirichlet-based evidence learning, our method is able to predict matching, unmatching and uncertainty scores of a pair of retrieved features. As a result, our method is able to determine whether they are from the same identity. Note that our method does not need to re-train the backbone networks and thus can be easily applied to different backbones and other similar tasks.

In Bayesian inference, placing prior distributions over deep models to estimate uncertainty has been widely explored [56], [57], e.g. Evidential Deep Learning (EDL) [2] and Prior Networks [58], [59] place Dirichlet priors over discrete classification predictions. Motivated by this, we employ the theoretical framework of EDL to model the probability distribution.

Given an input feature \mathbf{x} , EDL first uses an evidence collector to generate the evidence $\mathbf{e} = \{e_k | k = 1, \dots, K\}$, where K is the number of classes and e_k denotes the evidence of the k -th class. Based on the Subjective Logic theory [2], the evidence \mathbf{e} corresponds to a Dirichlet distribution parameterized by $\boldsymbol{\alpha} = \{\alpha_k | k = 1, \dots, K\}$, where $\alpha_k = e_k + 1$. A Dirichlet distribution is a probability density function for all the possible values of a probability mass function \mathbf{p} , and can be represented as:

$$\mathbf{D}(\mathbf{p} | \boldsymbol{\alpha}) = \begin{cases} \frac{1}{B(\boldsymbol{\alpha})} \prod_{i=1}^K p_i^{\alpha_i - 1} & \text{for } \mathbf{p} \in \mathcal{S}_K, \\ 0 & \text{otherwise,} \end{cases} \quad (1)$$

where $\mathcal{S}_K = \{\mathbf{p} | \sum_{i=1}^K p_i = 1 \text{ and } 0 \leq p_1, \dots, p_K \leq 1\}$ is the K -dimensional unit simplex, and $B(\boldsymbol{\alpha})$ is the K -dimensional multinomial beta function [60]. Here, p_k is the expected probability for the k -th class and is calculated as $p_k = \frac{\alpha_k}{S}$, where $S = \sum_{i=1}^K \alpha_i$.

We denote the ground-truth label of \mathbf{x} is \mathbf{y} that is a K -dimensional one-hot vector with $y_i = 1$ and $y_k = 0$ for all $k \neq i$. The Mean Square Error (MSE) is employed to measure the differences between the estimated class probabilities and the ground truth and can be expressed as:

$$\begin{aligned} \mathcal{L}_m(\Theta) &= \int \|\mathbf{y} - \mathbf{p}\|_2^2 \mathbf{D}(\mathbf{p} | \boldsymbol{\alpha}) \\ &= \sum_{i=1}^K (y_i^2 - 2y_i \mathbb{E}[p_i] + \mathbb{E}[p_i^2]), \end{aligned} \quad (2)$$

where \mathbb{E} indicates the expectation operation.

Furthermore, if an input feature cannot be correctly classified, its evidence ideally should shrink to zero. In other words, the Dirichlet distribution will be a uniform Dirichlet distribution. To this end, Sensoy et al. [2] introduce a Kullback-Leibler (KL) divergence term. As a result, the total loss function is represented as:

$$\mathcal{L}(\Theta) = \mathcal{L}_m(\Theta) + \lambda_t KL[\mathbf{D}(\mathbf{p} | \tilde{\boldsymbol{\alpha}}) \|\mathbf{D}(\mathbf{p} | \langle 1, \dots, 1 \rangle)], \quad (3)$$

where $\lambda_t = \min(1.0, t/10) \in [0, 1]$ is the annealing coefficient. $\mathbf{D}(\mathbf{p} | \langle 1, \dots, 1 \rangle)$ indicates a uniform Dirichlet distribution, t is the index of the current training iteration, and $\tilde{\boldsymbol{\alpha}} = \mathbf{y} + (1 - \mathbf{y}) \odot \boldsymbol{\alpha}$ is the Dirichlet parameters after the removal of the non-misleading evidence from predicted parameters $\boldsymbol{\alpha}$ for the input feature \mathbf{x} .

3.2 Uncertainty Modelling for Gait Recognition

As aforementioned, the premise that the gallery must contain an identity corresponding to the probe sample is considerably difficult to satisfy in practice, and OOD query cases may more likely happen if the gallery size is limited. Therefore, a mechanism to tackle OOD gait recognition is highly desirable.

A simple solution to this problem is to develop a binary classifier that classifies whether a probe sample and a gallery sample that has the minimum distance to the probe feature belong to the same identity. Here, the errors from the gait recognition networks should not affect the classifier performance as the adopted networks already achieve appealing performance on the gait feature representation. Using the simple classifier, the result of each retrieve can be formulated as:

$$Y = \begin{cases} OOD & F_c(q_i, g_j) \leq 0.5, \\ ID & F_c(q_i, g_j) > 0.5, \end{cases} \quad (4)$$

where Y is the framework output. OOD indicates the input probe feature q_i and gallery feature g_j are from different identities. ID represents the input probe feature q_i and gallery feature g_j are from the same identity. $F_c(\cdot)$ denotes a binary classifier that takes a probe feature and a gallery feature as input. Unfortunately, a simple binary classifier tends to output an over-confident erroneous prediction especially when an OOD query is fed into it. Hence, a classifier would fail to detect the OOD query and thus the gait recognition methods would assign incorrect identities to probes.

To address this problem, we introduce the theory of Evidential Deep Learning (EDL) [2] into current gait recognition tasks and then model the uncertainty of whether the query and retrieved features are from the same identity. The EDL theory is built on the Dempster-Shafer Theory of Evidence (DST), a generalization of the Bayesian theory to subjective probabilities [61]. To be specific, EDL assigns belief masses (e.g., probabilities) to a set of mutually exclusive labels, e.g., class labels for a sample. A belief mass can be assigned to any subset of a frame [61], including the whole frame itself. Here, the frame refers to the possible labels for a

sample. Different from traditional binary classification, we can introduce a label “I do not know” into the frame, representing the uncertainty to a given sample based on the theoretical framework of EDL. To formulate the belief mass assignments, Subjective Logic (SL) is an effective tool. Specifically, SL can formalize the belief assignments over a frame of discernment via a Dirichlet distribution. Thus, SL allows us to employ the principles of evidential theory to quantify the belief masses and uncertainty.

Driven by SL, we propose an uncertainty-aware gait recognition model that enables us to recognize ID and OOD queries in a unified framework (seeing Figure 2). In order to apply the uncertainty modeling of SL to our method, we first employ a gait recognition network to retrieve a gallery feature that has the minimum distance to the probe feature, and then compute the feature discrepancy between the probe and gallery features, called *residual feature*. Instead of directly measuring whether a query is OOD, we opt to examine the distribution of residual features. This is because modeling the gallery feature distribution explicitly is intractable.

Modeling the gallery distribution implicitly via a discriminator will degenerate into the case of learning a simple classifier, which has been demonstrated ineffective for the gait recognition problem. In contrast, the label space for a residual feature only contains *OOD* and *ID*, which is also much smaller than the identity number of the gallery set. In accordance with SL, we provide a belief mass b_k to the $K = 2$ labels (*e.g.*, b_1 indicates the probability of a matching pair, and b_2 indicates the probability of an unmatching pair) and an overall uncertainty mass μ . These 3 mass values are all non-negative and sum up to 1:

$$\mu + \sum_{k=1}^K b_k = 1. \quad (5)$$

Therefore, the retrieval result is determined by:

$$Y = \begin{cases} OOD & b_2 + \mu \geq b_1, \\ ID & b_2 + \mu < b_1. \end{cases} \quad (6)$$

When the prediction score of the matching class b_1 is higher than the sum of the score of the unmatching class b_2 and the uncertainty score, we believe the retrieved identity should be assigned to the probe. Otherwise, we will discard the retrieved identity as the probe sample could be an OOD query. Thanks to the uncertainty modeling of SL, we can effectively refuse OOD queries without harming the overall recognition performance.

3.3 Evidence Collector Design

In Eqn. (5), the mass values of b_k and μ are derived from the evidence ($e_k \geq 0$) and the evidence will be used to determine the Dirichlet distribution and uncertainty. Based on EDL, the evidence is a measure of support collected from data in favor of a sample to be classified into a certain class. Therefore, we develop a simple Multi-Layer Perceptron (MLP), including two fully-connected (FC) layers, to collect the evidence. That means the output of MLP is the evidence $e = \{e_k | k = 1, \dots, K\}$, where e_k denotes the evidence of the k -th class. To ensure the value of the evidence is non-negative, we adopt the ReLU function to filter the negative value. Once we obtain evidence e_k , the belief mass b_k and uncertainty mass μ are expressed as:

$$b_k = \frac{e_k}{S} \quad \text{and} \quad \mu = \frac{K}{S}, \quad (7)$$

where $S = \sum_{i=1}^K (e_i + 1)$. According to SL, a belief mass assignment corresponds to a Dirichlet distribution with parameters $\alpha_k = e_k + 1$ and $S = \sum_{i=1}^K \alpha_i$ is the Dirichlet strength. Eqn. (7) can be written as:

$$b_k = \frac{\alpha_k - 1}{\sum_{i=1}^K \alpha_i} \quad \text{and} \quad \mu = \frac{K}{\sum_{i=1}^K \alpha_i}. \quad (8)$$

Eqn. (8) implies if the strength of a Dirichlet distribution or evidence is larger, the Dirichlet distribution is more concentrated and the uncertainty of the prediction will become smaller. At that point, the prediction of the network will be more reliable. If evidence is lower (*i.e.*, the probabilities assigned to the two classes are small), the Dirichlet distribution will be flatter and the uncertainty of the prediction will be higher. Thus, the input might come from an OOD query.

3.4 Query Pair Construction

Our uncertainty-aware classification model aims to determine whether a pair of retrieved features are from the same identity or not. To train our classification model, we need to simulate the testing input. For this purpose, we construct pairs of samples, including positive and negative pairs. To be specific, a positive pair is obtained by sampling different sequences from the same identity, while we sample two sequences from different identities to construct a negative pair.

A simple strategy is to construct positive and negative pairs by randomly selecting two samples from the training set. Here, negative pairs are randomly chosen from two identities and positive pairs are randomly selected within the same identity. Even though we balance the number of positive and negative pairs, we find the network cannot effectively classify hard negative pairs. This is because the constructed pairs contain numerous simple cases that can be distinguished easily. In other words, our model does not have many chances to learn uncertain cases during training.

Inspired by the hard mining strategies, we construct the hardest positive and the hardest negative pairs within each training batch and thus enforce our model to classify highly uncertain samples. To be specific, we first randomly select P identities from the training set and then randomly choose V samples from each identity. Therefore, a total of $P \times V$ samples can be selected. Denote $I = \{f_{(1,1)}, f_{(1,2)}, \dots, f_{(i,j)}, \dots, f_{(P,V)}\}$ be the features of all selected samples. (i, j) indicates the j -th samples of the i -th identity. For the feature $f_{(i,j)}$, we can calculate the Euclidean distance between $f_{(i,j)}$ and each feature in I . Finally, the hardest positive pair can be constructed as $\langle f_{(i,j)}, f_{(i,q)} \rangle$, where $f_{(i,q)}$ has the maximum distance with the feature $f_{(i,j)}$ for all samples in the i -th identity. The hardest negative pair can be constructed as $\langle f_{(i,j)}, f_{(v,w)} \rangle$, where $f_{(v,w)}$ has the minimum distance with the feature $f_{(i,j)}$ and $v \neq i$. For all the features of I in the batch, we can totally generate $P \times V$ hardest positive pairs and $P \times V$ hardest negative pairs.

3.5 Inference

The inference stage of the uncertainty-aware gait recognition framework is shown in Figure 3. We first use a gait backbone to extract all the probe and gallery features. Recall $\mathbb{Q} = \{q_1, q_2, \dots, q_M\}$ denotes all the probe features from the probe set and $\mathbb{G} = \{g_1, g_2, \dots, g_N\}$ represents all the gallery features from the gallery set. For a probe feature q_i , we compute the distances

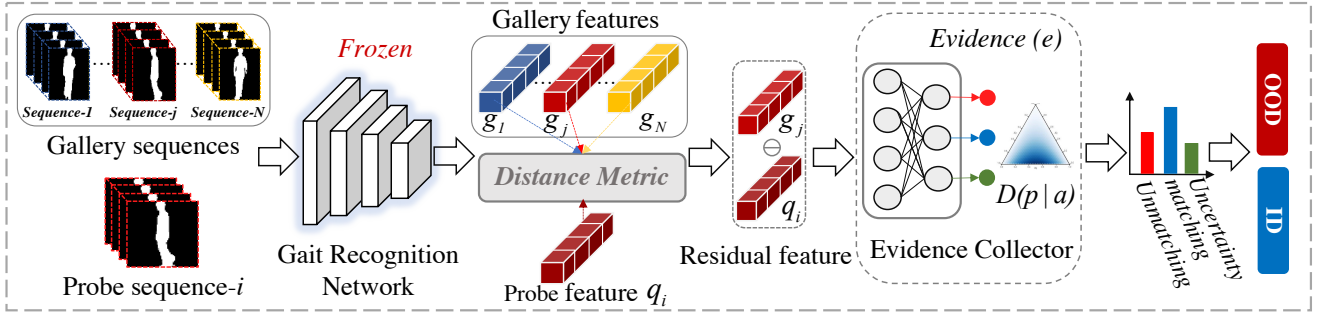


Fig. 3. Inference for the uncertainty-aware gait recognition framework. Given a probe feature q_i , we first search a gallery feature g_j that has the minimum distance to it, and then feed the two features to our evidence collector to determine in-distribution and out-of-distribution queries.

between q_i and all the gallery features and then find a gallery feature g_j that has the minimum distance to the probe.

Different from existing methods that assign the identity of g_j to the probe sample i , we utilize our uncertainty-aware gait recognition model to further determine whether the two features are from the same identity. To be specific, we compute the feature discrepancy between the two features, expressed by x . The feature discrepancy x is then fed into our uncertainty-aware gait recognition model to generate evidence $e = \{e_1, e_2\}$. From Eqn. (7), we can obtain the matching probability b_1 , the unmatching probability b_2 and the uncertainty probability μ . Based on the three probabilities and Eqn. (6), we can determine the identity of the probe sample i .

4 EXPERIMENTS

4.1 Dataset

We evaluate the effectiveness of our method on three gait recognition benchmarks OUMVLP [6], CASIA-B [62] and Gait3D [11]. Moreover, to verify the applicability of our method to other tasks, we also conduct experiments on other similar tasks, such as vehicle re-identification [63], [64] and synthetic person-identification benchmark VC-Clothes [65]. The details of these datasets are depicted as follows.

OUMVLP [6] is a large-scale gait dataset. It includes 10,307 subjects, each of which contains a gallery set and a probe set. Each subject in a set is collected from 14 views (0° - 90° and 180° - 270° with a sampling interval of 15°). In this work, we use the evaluation protocol [66], [67], [68] to verify the effectiveness of the proposed uncertainty-aware gait recognition method. Under the default evaluation protocol, 7% of the probes are OOD queries, which brings a challenge to the state-of-the-art methods. In addition, we manually remove some gallery sets of subjects to construct more severe OOD query scenarios.

CASIA-B [62] is one of the most popular gait datasets. It includes 124 subjects and about 1.3K sequences. Each subject is collected in sequences from 11 views ($0^\circ, 18^\circ, \dots, 180^\circ$). For each view, 10 groups of sequences are collected. In our experiments, the CASIA-B dataset is divided into three subsets: a training set, a query set, and a gallery set. To be specific, 74 IDs¹ are used to construct the training set and the remaining 50 IDs are used as the query and gallery sets. We select one image from each ID as the gallery set

and the rest images as the query set. By removing IDs from the gallery set, we construct various OOD query cases.

Gait3D [11] is a large-scale and in-the-wild dataset. It includes 4K subjects and 25K sequences captured by 39 surveillance cameras in the wild. In our experiments, the Gait3D dataset is divided into three subsets: a training set, a query set, and a gallery set. To be specific, 3,000 IDs² are used to construct the training set and the remaining 1,000 IDs are used as the query and gallery sets. We select one image from each ID as the query set and the rest images as the gallery set. By removing IDs from the gallery set, we construct various OOD query cases. Note that, in the default evaluation protocol, 5% of the probes are OOD queries. Moreover, we manually remove some subjects in the gallery set to construct more severe OOD query scenarios.

VERI-Wild [63], [64] is a large-scale dataset used for vehicle re-identification tasks. It includes 416,314 images captured by 174 surveillance cameras in the wild. In general, the VERI-Wild dataset is divided into three subsets: a training set, a query set, and a gallery set. We use the evaluation protocol as in [69], which includes three different settings, *i.e.*, Small-size Setting (SS), Medium-size Setting (MS) and Large-size Setting (LS). In the three settings, 3,000 IDs, 5,000 IDs and 10,000 IDs are used to construct the query and gallery sets, respectively. In each setting, we select one image from each ID as the gallery set and the rest images as the probe set. By removing IDs from the gallery set or probe set, we construct various OOD query cases.

VC-Clothes [65] is a synthetic person re-identification dataset. It includes 512 subjects and each subject has 36 corresponding images. The dataset has been divided into two subsets: a training set and a testing set. Each set contains 256 IDs. In the inference stage, we randomly choose four images from each subject for the gallery set and the rest images are used in the probe set. Hence, the gallery and probe sets contain 1020 images and 8591 images, respectively. Since we construct OOD queries on both OUMVLP, CASIA-B and Gait3D datasets, we will release all OOD configurations for reproducibility.

4.2 Implementation Details

Our uncertainty-aware classification model is built on multilayer perceptron (MLP) including two FC layers. For the OUMVLP dataset, we take three common gait recognition frameworks, GaitGL [68], GaitPart [67], GaitSet [66], OpenGait [70] and

1. Here, ID refers to identity. With a slight abuse of notation, we refer ID to as in-distribution for simplicity.

2. Here, ID refers to identity. With a slight abuse of notation, we refer ID to as in-distribution for simplicity.

TABLE 1

Rank-1 accuracy (%) on the OUMVLP dataset under different OOD percentages. The standard deviation is shown in parentheses. For a fair comparison, we join the backbones with different OOD detection strategies, e.g., Naive CLS, Verification and Anomaly Detection. Here, in the default evaluation protocol, 7% of the probes are OOD queries.

Methods	Different OOD percentages					
	7%	15%	25%	35%	45%	55%
GaitSet	87.34	79.71	70.35	61.80	52.29	42.73
GaitSet + Naive CLS	88.43 (\pm 0.00)	83.09 (\pm 0.00)	76.94 (\pm 0.00)	71.86 (\pm 0.02)	67.00 (\pm 0.07)	63.28 (\pm 0.06)
GaitSet + Verification	87.37 (\pm 0.00)	80.53 (\pm 0.01)	72.26 (\pm 0.02)	64.85 (\pm 0.02)	56.83 (\pm 0.02)	49.22 (\pm 0.03)
GaitSet + Anomaly Detection	87.85 (\pm 0.00)	81.24 (\pm 0.03)	73.39 (\pm 0.03)	66.58 (\pm 0.02)	59.54 (\pm 0.06)	53.40 (\pm 0.06)
GaitSet + Ours	88.14 (\pm 0.00)	86.64 (\pm 0.03)	85.16 (\pm 0.02)	84.26 (\pm 0.03)	83.84 (\pm 0.06)	84.09 (\pm 0.03)
GaitPart	88.80	80.97	71.39	62.65	52.96	43.23
GaitPart + Naive CLS	90.38 (\pm 0.00)	85.78 (\pm 0.02)	80.64 (\pm 0.02)	76.49 (\pm 0.05)	72.71 (\pm 0.06)	70.05 (\pm 0.08)
GaitPart + Verification	88.72 (\pm 0.00)	81.88 (\pm 0.01)	73.65 (\pm 0.02)	66.37 (\pm 0.01)	58.54 (\pm 0.03)	51.16 (\pm 0.02)
GaitPart + Anomaly Detection	89.66 (\pm 0.00)	83.50 (\pm 0.01)	76.33 (\pm 0.01)	70.22 (\pm 0.02)	64.15 (\pm 0.11)	59.11 (\pm 0.10)
GaitPart + Ours	89.88 (\pm 0.00)	88.41 (\pm 0.01)	86.96 (\pm 0.03)	86.03 (\pm 0.06)	85.53 (\pm 0.01)	85.68 (\pm 0.01)
GaitGL	90.17	82.15	72.35	63.45	53.58	43.68
GaitGL + Naive CLS	92.27 (\pm 0.00)	88.81 (\pm 0.01)	84.99 (\pm 0.03)	82.02 (\pm 0.05)	79.51 (\pm 0.05)	77.87 (\pm 0.08)
GaitGL + Verification	90.47 (\pm 0.00)	83.06 (\pm 0.00)	74.14 (\pm 0.02)	66.19 (\pm 0.02)	57.67 (\pm 0.06)	49.52 (\pm 0.07)
GaitGL + Anomaly Detection	91.53 (\pm 0.00)	86.21 (\pm 0.02)	80.15 (\pm 0.05)	75.15 (\pm 0.06)	70.43 (\pm 0.05)	66.77 (\pm 0.09)
GaitGL + Ours	91.52 (\pm 0.00)	90.27 (\pm 0.01)	89.03 (\pm 0.03)	88.21 (\pm 0.04)	87.82 (\pm 0.02)	87.87 (\pm 0.05)
GaitBase	92.88	84.91	74.65	64.94	54.96	44.81
GaitBase + Naive CLS	96.35 (\pm 0.00)	92.47 (\pm 0.02)	88.21 (\pm 0.01)	84.90 (\pm 0.02)	82.01 (\pm 0.05)	80.26 (\pm 0.05)
GaitBase + Verification	97.24 (\pm 0.00)	94.74 (\pm 0.03)	92.02 (\pm 0.03)	89.80 (\pm 0.02)	87.76 (\pm 0.03)	86.32 (\pm 0.02)
GaitBase + Anomaly Detection	94.83 (\pm 0.00)	88.85 (\pm 0.01)	82.06 (\pm 0.04)	76.43 (\pm 0.02)	71.06 (\pm 0.05)	67.04 (\pm 0.07)
GaitBase + Ours	98.63 (\pm 0.00)	97.48 (\pm 0.01)	96.33 (\pm 0.00)	95.50 (\pm 0.02)	94.93 (\pm 0.03)	94.73 (\pm 0.00)
DyGait	92.94	84.96	74.68	64.97	54.98	44.82
DyGait + Naive CLS	97.30 (\pm 0.00)	94.48 (\pm 0.05)	91.51 (\pm 0.01)	89.29 (\pm 0.03)	87.48 (\pm 0.07)	86.61 (\pm 0.04)
DyGait + Verification	97.28 (\pm 0.00)	94.19 (\pm 0.06)	90.74 (\pm 0.05)	87.89 (\pm 0.05)	85.28 (\pm 0.06)	83.41 (\pm 0.08)
DyGait + Anomaly Detection	95.60 (\pm 0.00)	90.61 (\pm 0.05)	85.11 (\pm 0.04)	80.72 (\pm 0.07)	76.83 (\pm 0.02)	74.29 (\pm 0.04)
DyGait + Ours	99.00 (\pm 0.00)	98.13 (\pm 0.04)	97.26 (\pm 0.01)	96.65 (\pm 0.02)	96.20 (\pm 0.03)	96.08 (\pm 0.02)

DyGait [5], as the backbones to extract gait features and evaluate the effectiveness of our proposed uncertainty-aware classification model. Since the feature sizes of the five backbones are different, we set the hidden layer size of our MLP to 544, 544, 768, 768 and 769, respectively. For the CASIA-B dataset, the MLP hidden layer size of five frameworks is set to 8192. For the Gait3D dataset, we also take the five frameworks as the backbones to extract gait features and evaluate the effectiveness of our proposed uncertainty-aware classification model. We set the hidden layer size of our MLP to 8192. For the VERI-Wild dataset, BoT [71] is used as the backbone and thus the hidden layer size of MLP of the uncertainty-aware classification model is set to 1024. For the VC-clothes dataset, we take CBN [72] as the backbone and the hidden layer size of MLP is set to 4096.

In Sec. 3.4, we propose a sampling strategy that constructs positive and negative pairs of samples to train our model. The proposed sampling strategy includes two hyper-parameters P and V . P and V are set to 32 and 8 respectively for all the experiments. The learning rate is set to $1e-3$ and then decays by a factor of 0.1 every 10 iterations. The total training iteration number for all the experiments is set to 50. In our experiments, we also run each OOD setting by three times in order to demonstrate the robustness of our method against OOD queries. Specifically, in each OOD setting, we randomly remove a certain percentage of the identities of the original gallery set three times to construct a different

gallery set. We will release our training details and codes.

4.3 Comparisons with the State-of-the-art

Evaluation on OUMVLP under different OOD percentages:

We introduce our uncertainty-aware classification model to several state-of-the-art gait recognition models, including GaitGL [68], GaitPart [67], GaitSet [66], OpenGait [70] and DyGait [5] on OUMVLP, and compare them with/without employing our method. In the experiments, we run five gait recognition models on six test sets with different percentages of OOD samples. As indicated in Table 1, after introducing our method, all of the gait recognition models obtain improvements on the test sets with OOD samples. As the percentage of OOD samples increases in the test sets, we observe that existing methods suffer severe performance degradation. As expected, when the OOD query rate reaches 50%, the accuracy of current methods almost decreases to half of their original performance (from 92.94% to 44.82% for DyGait). This implies that current gait recognition methods do not have the ability to detect OOD probes. On the contrary, our uncertainty-aware classification model is able to identify the OOD queries and thus avoids assigning gallery IDs to the probes. As a result, our method maintains high recognition accuracy while successfully recognizing OOD probes. This indicates the effectiveness and superiority of our proposed method. Moreover, the

TABLE 2

Rank-1 accuracy (%) on the CASIA-B dataset under different OOD percentages. The standard deviation is shown in parentheses. For a fair comparison, we join the backbones with different OOD detection strategies, e.g., Naive CLS, Verification and Anomaly Detection.

Methods	Different OOD percentages					
	0%	15%	25%	35%	45%	55%
GaitSet	91.81	79.39	70.92	63.23	53.22	42.53
GaitSet + Naive CLS	91.78 (± 0.00)	81.77 (± 0.87)	74.10 (± 1.06)	66.89 (± 1.46)	61.05 (± 1.98)	55.18 (± 0.62)
GaitSet + Verification	83.31 (± 0.00)	78.22 (± 0.55)	71.89 (± 0.48)	70.39 (± 1.12)	68.45 (± 1.76)	66.85 (± 1.59)
GaitSet + Anomaly Detection	91.72 (± 0.00)	81.69 (± 0.79)	74.78 (± 0.89)	68.17 (± 1.91)	62.30 (± 1.43)	55.34 (± 1.00)
GaitSet + Ours	91.38 (± 0.00)	83.25 (± 1.13)	76.55 (± 0.77)	71.80 (± 1.80)	68.94 (± 3.62)	63.12 (± 2.25)
GaitPart	92.61	80.16	72.19	63.63	53.81	44.20
GaitPart + Naive CLS	91.38 (± 0.00)	81.10 (± 0.75)	73.44 (± 1.16)	66.95 (± 0.22)	61.47 (± 1.23)	56.70 (± 1.13)
GaitPart + Verification	81.00 (± 0.00)	74.96 (± 0.79)	68.28 (± 0.80)	66.84 (± 1.25)	65.36 (± 1.42)	65.46 (± 0.92)
GaitPart + Anomaly Detection	91.59 (± 0.00)	79.49 (± 0.55)	70.95 (± 0.97)	63.04 (± 0.82)	55.59 (± 1.18)	49.45 (± 1.33)
GaitPart + Ours	90.94 (± 0.00)	81.80 (± 0.37)	74.93 (± 0.64)	70.00 (± 1.00)	66.22 (± 1.63)	61.88 (± 1.94)
GaitGL	94.77	81.89	73.27	64.50	54.74	44.01
GaitGL + Naive CLS	94.47 (± 0.00)	85.10 (± 1.17)	77.27 (± 1.02)	71.71 (± 1.28)	66.38 (± 0.58)	59.90 (± 0.59)
GaitGL + Verification	32.00 (± 0.00)	41.62 (± 0.14)	47.98 (± 0.78)	54.79 (± 0.63)	61.42 (± 0.047)	68.33 (± 0.60)
GaitGL + Anomaly Detection	94.77 (± 0.00)	83.55 (± 0.56)	74.91 (± 0.70)	66.62 (± 1.46)	58.58 (± 1.26)	48.93 (± 0.75)
GaitGL + Ours	93.79 (± 0.00)	85.61 (± 1.08)	79.06 (± 0.92)	74.83 (± 1.52)	70.96 (± 0.61)	65.83 (± 0.27)
GaitBase	96.01	82.97	74.11	64.44	54.64	44.82
GaitBase + Naive CLS	95.89 (± 0.00)	84.69 (± 0.29)	77.65 (± 1.29)	69.71 (± 0.54)	63.37 (± 1.80)	57.36 (± 0.65)
GaitBase + Verification	96.01 (± 0.00)	82.89 (± 0.57)	73.78 (± 0.66)	64.42 (± 0.65)	55.32 (± 0.15)	47.02 (± 1.06)
GaitBase + Anomaly Detection	95.89 (± 0.00)	84.36 (± 0.31)	77.05 (± 1.07)	68.75 (± 0.36)	62.10 (± 1.70)	55.44 (± 0.51)
GaitBase + Ours	95.45 (± 0.00)	86.75 (± 0.75)	81.53 (± 1.36)	76.20 (± 0.69)	72.43 (± 2.45)	68.62 (± 2.78)
DyGait	97.28	84.05	74.94	64.41	54.47	44.56
DyGait + Naive CLS	97.28 (± 0.00)	86.22 (± 0.32)	77.66 (± 0.31)	70.75 (± 0.88)	63.67 (± 0.75)	57.26 (± 1.02)
DyGait + Verification	42.53 (± 0.00)	50.95 (± 0.29)	56.66 (± 0.88)	62.23 (± 1.50)	67.79 (± 1.10)	73.88 (± 1.25)
DyGait + Anomaly Detection	97.28 (± 0.00)	86.23 (± 0.37)	77.68 (± 0.33)	70.46 (± 0.96)	63.16 (± 0.51)	56.29 (± 0.76)
DyGait + Ours	95.76 (± 0.00)	89.38 (± 0.35)	85.06 (± 0.89)	83.36 (± 1.76)	81.66 (± 1.42)	77.98 (± 1.48)

small standard deviation of our results demonstrates the stability of our model in recognizing OOD samples.

Evaluation on CASIA-B under different OOD percentages:

For the CASIA-B dataset, we also choose GaitGL [68], GaitPart [67], GaitSet [66], OpenGait [70] and DyGait [5] as our baseline algorithms. Table. 2 shows the experimental results. It can be observed that our method decreases slightly performance without OOD (from 97.28% to 95.76% for DyGait). This is because our method is prone to ensure the found matching pairs to be correct with minimal risk. In contrast, our method achieves promising performance in all OOD cases. To be specific, the accuracy of DyGait without our uncertainty model decreases significantly as the percentage of OOD samples increases (from 97.28% to 44.56% for GaitGL), while our method outperforms the baseline method for the six OOD percentages.

Evaluation on Gait3D under different OOD percentages: For the Gait3D dataset, we choose GaitGL [68], GaitPart [67], GaitSet [66], OpenGait [70] and DyGait [5] as our baseline backbones. Table 3 shows the experimental results. It can be observed that our method achieves a significant performance improvement in all cases. For instance, in the 55% OOD percentage, our method outperforms DyGait by 36.31%. Although our method still achieves a significant performance improvement in all OOD percentages, it suffers performance degradation in the 5% OOD percentage for GaitSet and GaitPart backbones. The main reason is that previous SOTA methods cannot effectively extract discriminative features

on Gait3D (the accuracy of SOTA methods is lower than 55%). When the extracted features are not sufficiently discriminative, in handling in-distribution queries, our method tends to be inaccurate. This is because, in such cases, the distance between a matching pair is large, leading to a higher risk. Meanwhile our network prefers to accept matching pairs with minimal risk.

Evaluation on VERI-Wild and VC-Clothes under different OOD percentages: Although our model is designed to tackle OOD queries in gait recognition, it can be easily extended to other tasks, such as vehicle re-identification and person re-identification. To further verify the effectiveness of our method on other tasks, we conduct experiments on VERI-Wild and VC-Clothes.

For the VERI-Wild dataset, we choose the BoT framework [71] as our baseline algorithm. The experimental results are shown in Table 5. It can be observed that our method (BoT + Ours) achieves appealing performance in all cases. To be specific, our method achieves stable recognition accuracy for the five OOD percentages while outperforming the baseline method. In contrast, the accuracy of BoT without our uncertainty model decreases significantly as the percentage of OOD samples increases. For the VC-Clothes dataset, we employ the CBN framework [72] as our baseline algorithm. As indicated in Table 6, our methods achieve approximately more than 97% recognition accuracy in all the cases, *i.e.*, OOD percentage ranges from 15% to 55%. On the contrary, the recognition accuracy of CBN without our uncertainty model is 44.98% in the setting of 55% OOD samples.

TABLE 3

Rank-1 accuracy (%) on the Gait3D dataset under different OOD percentages. The standard deviation is shown in parentheses. For a fair comparison, we join the backbones with different OOD detection strategies, e.g., Naive CLS, Verification and Anomaly Detection. Note that, the default evaluation protocol contains 5% of the probes which are OOD queries.

Methods	Different OOD percentages					
	5%	15%	25%	35%	45%	55%
GaitSet	55.33	40.24	32.46	27.66	21.51	17.00
GaitSet + Naive CLS	54.27 (± 0.00)	43.26 (± 1.42)	40.12 (± 1.40)	41.59 (± 0.88)	43.67 (± 0.30)	45.72 (± 1.18)
GaitSet + Verification	55.33 (± 0.00)	42.36 (± 1.45)	34.38 (± 1.02)	29.79 (± 0.52)	26.41 (± 1.46)	24.46 (± 1.76)
GaitSet + Anomaly Detection	55.61 (± 0.00)	43.16 (± 0.94)	37.78 (± 0.73)	36.02 (± 1.02)	35.63 (± 0.48)	36.53 (± 0.97)
GaitSet + Ours	51.20 (± 0.00)	39.92 (± 0.84)	38.99 (± 0.56)	41.82 (± 0.93)	46.36 (± 0.95)	51.33 (± 0.95)
GaitPart	43.32	29.49	23.72	20.17	15.75	12.48
GaitPart + Naive CLS	39.09 (± 0.00)	30.86 (± 0.51)	31.54 (± 0.23)	33.33 (± 1.09)	37.01 (± 0.88)	38.97 (± 0.66)
GaitPart + Verification	43.41 (± 0.00)	30.93 (± 0.90)	24.94 (± 0.67)	21.61 (± 0.67)	19.24 (± 1.10)	17.29 (± 0.92)
GaitPart + Anomaly Detection	40.63 (± 0.00)	30.58 (± 1.20)	29.10 (± 0.89)	29.26 (± 0.71)	30.89 (± 0.73)	30.93 (± 0.69)
GaitPart + Ours	39.86 (± 0.00)	30.70 (± 0.84)	31.86 (± 0.32)	35.83 (± 0.55)	41.08 (± 0.71)	45.18 (± 1.53)
GaitGL	73.77	56.48	48.41	40.44	31.69	24.78
GaitGL + Naive CLS	73.87 (± 0.00)	58.59 (± 0.39)	53.05 (± 0.57)	48.22 (± 0.36)	46.46 (± 0.91)	45.18 (± 1.41)
GaitGL + Verification	72.04 (± 0.00)	56.80 (± 0.12)	50.24 (± 0.68)	45.02 (± 0.70)	42.55 (± 1.01)	40.28 (± 1.01)
GaitGL + Anomaly Detection	73.77 (± 0.00)	57.79 (± 0.53)	50.75 (± 0.87)	44.54 (± 0.36)	40.92 (± 1.60)	38.48 (± 1.00)
GaitGL + Ours	74.15 (± 0.00)	59.49 (± 1.58)	56.06 (± 0.89)	53.40 (± 1.49)	54.05 (± 0.82)	55.00 (± 0.80)
GaitBase	75.02	57.15	47.74	40.82	34.48	27.56
GaitBase + Naive CLS	73.29 (± 0.00)	60.13 (± 1.44)	55.20 (± 1.30)	54.24 (± 1.18)	55.30 (± 0.79)	57.05 (± 0.77)
GaitBase + Verification	74.92 (± 0.00)	59.39 (± 1.65)	49.88 (± 1.33)	42.26 (± 0.55)	36.40 (± 1.03)	32.46 (± 1.31)
GaitBase + Anomaly Detection	74.92 (± 0.00)	59.65 (± 1.69)	51.00 (± 1.23)	44.38 (± 0.47)	39.73 (± 0.53)	37.27 (± 1.41)
GaitBase + Ours	75.31 (± 0.00)	60.35 (± 1.11)	56.09 (± 1.26)	55.52 (± 1.54)	57.06 (± 0.75)	59.07 (± 0.14)
DyGait	75.98	62.05	52.25	45.43	37.46	30.45
DyGait + Naive CLS	76.46 (± 0.00)	65.96 (± 0.92)	60.39 (± 1.45)	58.69 (± 0.96)	59.42 (± 0.83)	61.54 (± 0.16)
DyGait + Verification	72.62 (± 0.00)	62.18 (± 0.73)	56.51 (± 1.20)	54.43 (± 0.25)	53.66 (± 1.14)	53.92 (± 0.71)
DyGait + Anomaly Detection	76.17 (± 0.00)	64.90 (± 0.74)	58.05 (± 1.22)	54.14 (± 1.39)	52.42 (± 1.89)	53.44 (± 1.16)
DyGait + Ours	76.27 (± 0.00)	66.92 (± 1.63)	62.91 (± 1.71)	62.76 (± 0.83)	64.48 (± 0.71)	66.76 (± 0.21)

This is because the current methods cannot address OOD queries and thus their methods only output erroneous recognition results. Note that, when we apply our method to the baseline methods, we do not need to re-train the baselines but treat them as off-the-shelf backbone networks. This also indicates that our method is able to effectively recognize matching feature pairs and OOD queries through its prediction and uncertainty modeling, thus demonstrating the superiority of our method to competing methods.

4.4 Ablation Study

To verify the effectiveness of our proposed components, *i.e.*, the uncertainty modeling and query construction, we conduct ablation studies on gait recognition.

Effectiveness of the uncertainty modeling: Since existing backbones cannot handle OOD cases, they cannot reach 100% accuracy in all OOD settings. For a fair comparison, we introduce different OOD detection strategies and join them with the gait backbone to construct baseline algorithms. As a result, the upper bound accuracy of the constructed baseline algorithms is 100%. The details of baseline algorithms are as follows:

Backbone + Naive CLS: An NN classifier is designed to classify whether two features are from the same identity or not. The classifier is trained by a binary cross-entropy loss and our constructed pairs. The difference between this classifier and our model is that our model has uncertainty modeling. Thus, our model not only classifies whether two features are from the same identity but also provides the uncertainty estimation of the prediction by a Dirichlet distribution parameterized over all the constructed training pairs, while a simple classifier only makes decisions based on its predicted labels since it only learns a classification boundary. The experimental results are shown in Table 1. As expected, without any mechanism to distinguish OOD queries, the performance degrades as the number of OOD samples increases. Although a simple classifier outperforms slightly our method in the 7% OOD percentage, we can see that a simple classifier still struggles to recognize OOD queries. This is because a simple classifier tends to overfit the in-distribution pairs. Thus, it may produce inaccurate predictions, when the input pairs of features are out-of-distribution.

Backbone + Verification: Setting a similarity threshold is another

TABLE 4

Rank-1 accuracy (%) on the OUMVLP dataset under different OOD percentages. The standard deviation is shown in parentheses. For a fair comparison, we join the backbones with different OOD detection strategies, e.g., Naive CLS, Verification and Anomaly Detection.

Methods	Different OOD percentages					
	7%	15%	25%	35%	45%	55%
GaitGL	90.17	82.15	72.35	63.45	53.58	43.68
GaitGL + Threshold=0.6	90.41 (\pm 0.00)	84.74 (\pm 0.01)	78.05 (\pm 0.03)	72.30 (\pm 0.03)	66.46 (\pm 0.12)	61.23 (\pm 0.12)
GaitGL + Threshold=0.7	73.08 (\pm 0.00)	74.21 (\pm 0.02)	75.72 (\pm 0.03)	77.24 (\pm 0.04)	79.21 (\pm 0.07)	81.35 (\pm 0.06)
GaitGL + Threshold=0.8	27.34 (\pm 0.00)	33.87 (\pm 0.02)	41.83 (\pm 0.02)	49.07 (\pm 0.00)	57.09 (\pm 0.03)	65.07 (\pm 0.05)
GaitGL + Threshold=0.9	9.42 (\pm 0.00)	17.56 (\pm 0.01)	27.52 (\pm 0.01)	36.57 (\pm 0.02)	46.56 (\pm 0.01)	56.51 (\pm 0.01)
GaitGL + Naive CLS	92.27 (\pm 0.00)	88.81 (\pm 0.01)	84.99 (\pm 0.03)	82.02 (\pm 0.05)	79.51 (\pm 0.05)	77.87 (\pm 0.08)
GaitGL + Verification	90.47 (\pm 0.00)	83.06 (\pm 0.00)	74.14 (\pm 0.02)	66.19 (\pm 0.02)	57.67 (\pm 0.06)	49.52 (\pm 0.07)
GaitGL + Anomaly Detection	74.07 (\pm 0.00)	75.63 (\pm 0.02)	77.58 (\pm 0.04)	79.42 (\pm 0.03)	81.57 (\pm 0.02)	83.79 (\pm 0.02)
GaitGL + Ours	91.52 (\pm 0.00)	90.27 (\pm 0.01)	89.03 (\pm 0.03)	88.21 (\pm 0.04)	87.82 (\pm 0.02)	87.87 (\pm 0.05)
DyGait	92.94	84.96	74.68	64.97	54.98	44.82
DyGait + Threshold=0.6	92.94 (\pm 0.00)	84.96 (\pm 0.00)	74.68 (\pm 0.00)	64.97 (\pm 0.00)	54.98 (\pm 0.00)	44.82 (\pm 0.00)
DyGait + Threshold=0.7	93.36 (\pm 0.00)	85.00 (\pm 0.01)	74.80 (\pm 0.02)	65.54 (\pm 0.03)	55.39 (\pm 0.01)	45.33 (\pm 0.02)
DyGait + Threshold=0.8	97.91 (\pm 0.00)	95.72 (\pm 0.06)	93.32 (\pm 0.04)	91.39 (\pm 0.02)	89.69 (\pm 0.05)	88.53 (\pm 0.04)
DyGait + Threshold=0.9	31.50 (\pm 0.00)	37.64 (\pm 0.03)	45.19 (\pm 0.02)	52.03 (\pm 0.05)	59.57 (\pm 0.03)	67.09 (\pm 0.05)
DyGait + Naive CLS	97.30 (\pm 0.00)	94.48 (\pm 0.05)	91.51 (\pm 0.01)	89.29 (\pm 0.03)	87.48 (\pm 0.07)	86.61 (\pm 0.04)
DyGait + Verification	97.28 (\pm 0.00)	94.19 (\pm 0.06)	90.74 (\pm 0.05)	87.89 (\pm 0.05)	85.28 (\pm 0.06)	83.41 (\pm 0.08)
DyGait + Anomaly Detection	95.60 (\pm 0.00)	90.61 (\pm 0.05)	85.11 (\pm 0.04)	80.72 (\pm 0.07)	76.83 (\pm 0.02)	74.29 (\pm 0.04)
DyGait + Ours	99.00 (\pm 0.00)	98.13 (\pm 0.04)	97.26 (\pm 0.01)	96.65 (\pm 0.02)	96.20 (\pm 0.03)	96.08 (\pm 0.02)

TABLE 5

Rank-1 accuracy (%) on the VERI-Wild dataset under different OOD percentages. The standard deviation is reported in parentheses. SS, MS and LS indicate 3K, 5K and 10K training IDs, respectively.

Setting	Methods	Different OOD percentages				
		15%	25%	35%	45%	55%
SS	BoT	74.07	66.02	57.86	49.40	40.90
	BoT + Naive CLS	69.26	66.76	64.81	63.25	62.82
	BoT + Verification	74.10	66.36	58.99	52.01	46.24
	BoT + Ours	78.19	76.34	75.09	74.71	75.34
MS	BoT	71.00	63.64	55.83	47.73	39.87
	BoT + Naive CLS	64.81	61.65	59.33	57.17	55.84
	BoT + Verification	70.85	63.34	55.86	48.17	41.04
	BoT + Ours	73.70	70.85	68.97	67.65	67.36
LS	BoT	65.58	58.65	51.54	44.15	36.82
	BoT + Naive CLS	59.25	56.28	53.39	50.99	49.15
	BoT + Verification	65.43	58.63	51.57	44.40	37.14
	BoT + Ours	67.45	64.14	61.25	59.07	57.92

straightforward way to address OOD cases. When the similarity between the probe and the closet sample from the gallery is smaller than the threshold, the probe will be regarded as an OOD query. In our cases, the threshold is calculated by Equal Error Rate (EER) from the verification setting. To be specific, we construct 20k gait pairs, including 10k paired samples and 10k unpaired samples. Then, we search for the best threshold leading to the lowest EER. Finally, the searched threshold is used to further determine whether two samples are from the same identity. We

TABLE 6

Rank-1 accuracy (%) on the VC-Clothes dataset under different OOD percentages. The standard deviation is reported in parentheses.

Methods	Different OOD percentages				
	15%	25%	35%	45%	55%
CBN	83.91	73.67	64.10	54.34	44.98
CBN + Verification	89.68	90.71	91.72	92.90	93.95
CBN + Threshold	87.96	80.93	75.74	72.00	69.17
CBN + Ours	97.11	97.15	97.29	97.58	97.70

will release the constructed gait pairs for reproducibility. Table 1 shows that the verification-based methods address a few OOD cases, leading to a slight performance improvement. For example, in the 15% OOD setting, ‘‘DyGait + Verification’’ outperforms DyGait by 9.23% on OUMVLP. However, the verification-based methods cannot handle most OOD cases. This is because most OOD queries are hard samples. Here, ‘‘hard’’ means the OOD query is very similar to the closet sample from the gallery set. In other words, its similarity is higher than the given threshold, leading to erroneous results.

Backbone + Anomaly Detection: One-Class Novelty Detection [73] is proposed to address OOD cases in recognition. It aims to classify all OOD cases into one class. Although it cannot be used directly in our task, we combine it with an NN classifier to detect our OOD cases. To be specific, we randomly construct in-distribution and out-of-distribution feature pairs to train an NN classifier. The trained classifier is then employed in feature matching to determine whether the retrieved gait pairs are the

same identity or not. The experimental results are shown in Table 1. It can be observed that one-class novelty detection effectively addresses a few OOD cases. For example, “DyGait + Anomaly Detection” outperforms DyGait by 2.66% when the OOD query rate is 5% on OUMVLP. However, in the 45% and 55% OOD settings, its performance decreases significantly. This is because one-class novelty detection tends to classify an in-distribution pair that has a large distance to OOD cases. As a result, the accuracy in low OOD percentage shows a significant decrease. On the contrary, our method maintains the recognition performance even though the rate of OOD samples is more than 50%. Our method successfully identifies OOD queries and assigns correct identities to in-distribution queries. We also conduct our experiments three times on different gallery sets. The small standard deviation values also prove the stability of our method.

Impacts of different thresholds: For a fair comparison, we introduce different OOD detection strategies. One of our used strategies is to set a similarity threshold. If the similarity between the probe and the closet sample from the gallery is smaller than the threshold, the probe will be regarded as an OOD query. In this paper, we introduce a verification setting to automatically calculate the threshold. Obviously, the threshold can be set manually. Thus, we conduct experiments on OUMVLP by manually searching all thresholds. The experimental results are shown in Table 4. When the given threshold is lower than 0.6, the threshold-based method cannot detect any OOD cases. Thus, the accuracy in these threshold settings is the same as the accuracy using only the backbone. We also observe that a low threshold for GaitGL achieves appealing performance when the OOD percentage is less than 25%, but it cannot effectively address the condition with higher OOD percentages. In contrast, a high threshold achieves promising performance in high OOD percentages ($\geq 35\%$). For the DyGait backbone, we find that only “Threshold = 0.8” achieves promising performance, while other threshold settings lead to significant performance degradation. These results indicate that it is difficult to choose a suitable threshold for different OOD percentages. Thus, the threshold-based methods are impractical. Furthermore, it can be found that our method outperforms the threshold-based methods in all OOD percentages and the recognition accuracy in all OOD percentages is stable. We believe that the proposed method is a more practical approach to addressing OOD queries in a real scene.

Impacts of different query pair construction: We propose an OOD query pair construction that allows our network to grasp the idea of in-distribution and OOD residual features. We also compare three different strategies: randomly selecting feature pairs, dataset-based hard negative and positive feature pairs, and batch-based hard negative and positive feature pairs. All experiments are conducted on OUMVLP and we take GaitGL as our backbone. As indicated in Figure 4, both random selection of feature pairs and batch-based hard negative and positive feature pair mining strategies improve the recognition performance on OOD cases in testing. Note that, as the percentage of the OOD queries increases, the performance of the model trained with random selection of feature pairs decreases. This is mainly because this pair construction may not effectively capture the most uncertain cases for model training. The dataset-based mining strategy does not facilitate the representation of the distribution of the residual features. In most cases, the negative feature pairs from the dataset-based mining strategy are hard to be classified and thus our classifier will exert more efforts to classify the negative pairs after training while

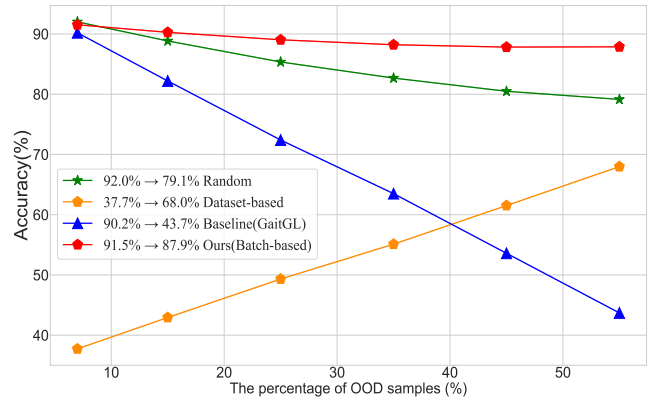


Fig. 4. Impacts of different query pair construction on training our model. We test the models with different percentages of OOD queries.

sacrificing the classification accuracy on positive pairs. Mining in a batch-based pair will significantly improve the variety of training samples, thus leading to better recognition performance. Thanks to our feature pair construction, we can effectively capture the latent distribution of residual features, thus achieving accurate detection of OOD samples.

5 DISCUSSION, LIMITATION AND EXTENSION

In this section, we further analyze the advantages and limitations of our proposed uncertainty gait recognition framework. Additionally, we extend our method to other tasks, *i.e.*, vehicle re-identification and person re-identification.

Performance of the default evaluation protocol: In this paper, we combine the backbone networks with different OOD detection strategies, including Naive CLS, Verification, and Anomaly Detection. Experimental results are reported in Table. 1, Table. 2 and Table. 3, respectively. Our method achieves a significant performance improvement in all OOD percentages, but it also suffers slight performance degradation in the in-distribution scenario. For example, in the default evaluation protocol on the OUMVLP dataset (with 7% OOD queries), the accuracy of GaitGL with our methods (91.52%) is lower than the accuracy of GaitGL with the Naive CLS (92.27%). We speculate the main reason is that the feature space of the three backbones (GaitSet, GaitPart and GaitGL) among different subjects is not discriminative enough (without sufficient margins/distance) for some hard cases and thus those samples will be rejected by our method. Since our method prefers to accept matching pairs with minimal risk, these high-risk predictions are rejected and the overall accuracy drops in the in-distribution case.

Performance across different datasets: We conduct experiments on three popular used datasets, CASIA-B, OUMVLP and Gait3D, to verify the effectiveness of our uncertainty gait recognition framework. Table. 1, Table. 2 and Table. 3 demonstrate state-of-the-art backbones with our methods achieve superior performance in all OOD percentages. Additionally, for the default setting on the OUMVLP dataset, DyGait with our method achieves an accuracy of 99.00%. When the OOD percentage increases to 55%, our method still obtains 96.08% Rank-1 accuracy. The performance degradation on the OUMVLP dataset is only 3%. However, there is an obvious performance degradation on the CASIA-B dataset when the OOD percentage increases from 0% to 55%. We speculate that our method trained on a small dataset,

like CASIA-B which only contains 74 subjects for training, may not learn sufficiently discriminative features and thus suffers a performance drop in high OOD percentage.

For the Gait3D dataset, it is observed that the performance degrades about 10% as OOD percentage increases from 5% to 55%. The main reason is that existing methods cannot effectively extract discriminative features on Gait3D (the accuracy of these methods is lower than 50%). When the extracted features are not discriminative in handling in-distribution queries, we do not expect these features to be robust enough to address OOD queries.

Extension to other tasks: To verify the applicability of our method to other tasks, we also conduct experiments on vehicle re-identification benchmark VERI-Wild [63], [64] and synthetic person-identification benchmark VC-Clothes [65]. The experimental details and results can be found in Table. 5 and Table. 6. These experiments demonstrate our uncertainty-aware model is able to effectively recognize matching feature pairs and OOD queries through its prediction and uncertainty modeling, thus demonstrating the superiority of our method to the SOTA methods.

6 CONCLUSION

In this paper, we propose a novel uncertainty-aware gait recognition model that can effectively identify whether a probe sample is out of the distribution of the gallery samples. To the best of our knowledge, our work is the first attempt to endow gait recognition with the capability to address OOD queries via uncertainty modeling. Furthermore, our proposed method is a unified framework that is not only able to address OOD query samples but also to successfully recognize the in-distribution samples. Since our method takes extracted gait features as input, it can be applied to various gait recognition networks, and thus agnostic against backbone networks. More importantly, our model can be generalized to other recognition tasks, such as vehicle and person re-identification, and improves the robustness to OOD queries, which frequently occur in practice.

ACKNOWLEDGMENTS

This work was supported by the ARC-Discovery grant (DP220100800) and ARC-DECRA grant (DE230100477), the National Natural Science Foundation of China (61976017 and 61601021), the Beijing Natural Science Foundation (4202056), the Fundamental Research Funds for the Central Universities (2022JBM013). The support and resources from the Center for High Performance Computing at Beijing Jiaotong University (<http://hpc.bjtu.edu.cn>) are gratefully acknowledged.

REFERENCES

- [1] C. Wan, L. Wang, and V. V. Phoha, "A survey on gait recognition," *ACM Computing Surveys (CSUR)*, vol. 51, no. 5, pp. 1–35, 2018.
- [2] M. Sensoy, L. Kaplan, and M. Kandemir, "Evidential deep learning to quantify classification uncertainty," *Advances in Neural Information Processing Systems*, vol. 31, 2018.
- [3] A. P. Dempster, "A generalization of bayesian inference," *Journal of the Royal Statistical Society: Series B (Methodological)*, vol. 30, no. 2, pp. 205–232, 1968.
- [4] A. Jsang, "Subjective logic: A formalism for reasoning under uncertainty," *Springer Verlag*, 2016.
- [5] M. Wang, X. Guo, B. Lin, T. Yang, Z. Zhu, L. Li, S. Zhang, and X. Yu, "Dyggait: Exploiting dynamic representations for high-performance gait recognition," in *Proceedings of the IEEE/CVF Conference on Computer Vision and Pattern Recognition*, 2023.
- [6] N. Takemura, Y. Makihara, D. Muramatsu, T. Echigo, and Y. Yagi, "Multi-view large population gait dataset and its performance evaluation for cross-view gait recognition," *IPSN Transactions on Computer Vision and Applications*, vol. 10, no. 1, p. 4, 2018.
- [7] A. Sepas-Moghaddam and A. Etemad, "Deep gait recognition: A survey," *IEEE Transactions on Pattern Analysis and Machine Intelligence*, 2022.
- [8] C. Shen, S. Yu, J. Wang, G. Q. Huang, and L. Wang, "A comprehensive survey on deep gait recognition: Algorithms, datasets and challenges," *arXiv preprint arXiv:2206.13732*, 2022.
- [9] S. Yu, Y. Huang, L. Wang, Y. Makihara, E. B. G. Reyes, F. Zheng, M. A. R. Ahad, B. Lin, Y. Yang, H. Xiong *et al.*, "Hid 2021: Competition on human identification at a distance 2021," in *2021 IEEE International Joint Conference on Biometrics (IJCB)*. IEEE, 2021, pp. 1–7.
- [10] Z. Zhu, X. Guo, T. Yang, J. Huang, J. Deng, G. Huang, D. Du, J. Lu, and J. Zhou, "Gait recognition in the wild: A benchmark," in *ICCV*, 2021.
- [11] J. Zheng, X. Liu, W. Liu, L. He, C. Yan, and T. Mei, "Gait recognition in the wild with dense 3d representations and a benchmark," in *Proceedings of the IEEE/CVF Conference on Computer Vision and Pattern Recognition*, 2022, pp. 20228–20237.
- [12] S. Zhang, Y. Wang, and A. Li, "Cross-view gait recognition with deep universal linear embeddings," in *Proceedings of the IEEE/CVF Conference on Computer Vision and Pattern Recognition*, 2021, pp. 9095–9104.
- [13] X. Li, Y. Makihara, C. Xu, and Y. Yagi, "Multi-view large population gait database with human meshes and its performance evaluation," *IEEE Transactions on Biometrics, Behavior, and Identity Science*, vol. 4, no. 2, pp. 234–248, 2022.
- [14] D. K. Wagg and M. S. Nixon, "On automated model-based extraction and analysis of gait," in *CAFGR*, 2004.
- [15] X. Li, Y. Makihara, C. Xu, Y. Yagi, S. Yu, and M. Ren, "End-to-end model-based gait recognition," in *ACCV*, 2020.
- [16] X. Li, Y. Makihara, C. Xu, and Y. Yagi, "End-to-end model-based gait recognition using synchronized multi-view pose constraint," in *Proceedings of the IEEE/CVF International Conference on Computer Vision*, 2021, pp. 4106–4115.
- [17] T. Teepe, A. Khan, J. Gilg, F. Herzog, S. Hörmann, and G. Rigoll, "Gait-graph: Graph convolutional network for skeleton-based gait recognition," in *2021 IEEE International Conference on Image Processing (ICIP)*. IEEE, 2021, pp. 2314–2318.
- [18] R. Liao, S. Yu, W. An, and Y. Huang, "A model-based gait recognition method with body pose and human prior knowledge," *Pattern Recognition*, vol. 98, p. 107069, 2020.
- [19] H.-M. Hsu, Y. Wang, C.-Y. Yang, J.-N. Hwang, H. L. U. Thuc, and K.-J. Kim, "Gaittake: Gait recognition by temporal attention and keypoint-guided embedding," in *2022 IEEE International Conference on Image Processing (ICIP)*. IEEE, 2022, pp. 2546–2550.
- [20] T. Teepe, J. Gilg, F. Herzog, S. Hörmann, and G. Rigoll, "Towards a deeper understanding of skeleton-based gait recognition," in *Proceedings of the IEEE/CVF Conference on Computer Vision and Pattern Recognition*, 2022, pp. 1569–1577.
- [21] K. Shiraga, Y. Makihara, D. Muramatsu, T. Echigo, and Y. Yagi, "Geinet: View-invariant gait recognition using a convolutional neural network," in *ICB*. IEEE, 2016, pp. 1–8.
- [22] X. Li, Y. Makihara, C. Xu, Y. Yagi, and M. Ren, "Gait recognition via semi-supervised disentangled representation learning to identity and covariate features," in *CVPR*, 2020.
- [23] X. Wang and W. Q. Yan, "Human gait recognition based on frame-by-frame gait energy images and convolutional long short-term memory," *IJNS*, 2020.
- [24] C. Shen, B. Lin, S. Zhang, G. Q. Huang, S. Yu, and X. Yu, "Gait recognition with mask-based regularization," *arXiv preprint arXiv:2203.04038*, 2022.
- [25] B. Lin, Y. Liu, and S. Zhang, "Gaitmask: Mask-based model for gait recognition." *BMVC*, 2021.
- [26] B. Lin, S. Zhang, and F. Bao, "Gait recognition with multiple-temporal-scale 3d convolutional neural network," in *Proceedings of the 28th ACM international conference on multimedia*, 2020, pp. 3054–3062.
- [27] T. Chai, A. Li, S. Zhang, Z. Li, and Y. Wang, "Lagrange motion analysis and view embeddings for improved gait recognition," in *Proceedings of the IEEE/CVF Conference on Computer Vision and Pattern Recognition*, 2022, pp. 20249–20258.
- [28] X. Huang, D. Zhu, H. Wang, X. Wang, B. Yang, B. He, W. Liu, and B. Feng, "Context-sensitive temporal feature learning for gait recognition," in *Proceedings of the IEEE/CVF International Conference on Computer Vision*, 2021, pp. 12909–12918.
- [29] B. Lin, S. Zhang, M. Wang, L. Li, and X. Yu, "Gaitgl: Learning discriminative global-local feature representations for gait recognition," *arXiv preprint arXiv:2208.01380*, 2022.

- [30] M. Wang, B. Lin, X. Guo, L. Li, Z. Zhu, J. Sun, S. Zhang, and X. Yu, "Gaitstrip: Gait recognition via effective strip-based feature representations and multi-level framework," *arXiv preprint arXiv:2203.03966*, 2022.
- [31] B. Lin, S. Zhang, Y. Liu, and S. Qin, "Multi-scale temporal information extractor for gait recognition," in *2021 IEEE International Conference on Image Processing (ICIP)*. IEEE, 2021, pp. 2998–3002.
- [32] W. Yu, H. Yu, Y. Huang, C. Cao, and L. Wang, "Cntr: Cyclic noise-tolerant network for gait recognition," *arXiv preprint arXiv:2210.06910*, 2022.
- [33] W. Yu, H. Yu, Y. Huang, and L. Wang, "Generalized inter-class loss for gait recognition," in *Proceedings of the 30th ACM International Conference on Multimedia*, 2022, pp. 141–150.
- [34] J. Liang, C. Fan, S. Hou, C. Shen, Y. Huang, and S. Yu, "Gaitedge: Beyond plain end-to-end gait recognition for better practicality," *arXiv preprint arXiv:2203.03972*, 2022.
- [35] H. Dou, P. Zhang, Y. Zhao, L. Dong, Z. Qin, and X. Li, "Gaitmpl: Gait recognition with memory-augmented progressive learning," *IEEE Transactions on Image Processing*, 2022.
- [36] H. Dou, P. Zhang, W. Su, Y. Yu, and X. Li, "Metagait: Learning to learn an omni sample adaptive representation for gait recognition," in *European Conference on Computer Vision*. Springer, 2022, pp. 357–374.
- [37] T. Huang, X. Ben, C. Gong, B. Zhang, R. Yan, and Q. Wu, "Enhanced spatial-temporal salience for cross-view gait recognition," *IEEE Transactions on Circuits and Systems for Video Technology*, 2022.
- [38] S. Hou, X. Liu, C. Cao, and Y. Huang, "Set residual network for silhouette-based gait recognition," *IEEE Transactions on Biometrics, Behavior, and Identity Science*, vol. 3, no. 3, pp. 384–393, 2021.
- [39] S. Hou, C. Cao, X. Liu, and Y. Huang, "Gait lateral network: Learning discriminative and compact representations for gait recognition," in *European conference on computer vision*. Springer, 2020, pp. 382–398.
- [40] Z. Huang, D. Xue, X. Shen, X. Tian, H. Li, J. Huang, and X.-S. Hua, "3d local convolutional neural networks for gait recognition," in *Proceedings of the IEEE/CVF International Conference on Computer Vision*, 2021, pp. 14 920–14 929.
- [41] X. Zhu, Z. Luo, P. Fu, and X. Ji, "Voc-reid: Vehicle re-identification based on vehicle-orientation-camera," in *Proceedings of the IEEE/CVF Conference on Computer Vision and Pattern Recognition Workshops*, 2020, pp. 602–603.
- [42] Z. Tang, M. Naphade, M.-Y. Liu, X. Yang, S. Birchfield, S. Wang, R. Kumar, D. Anastasiu, and J.-N. Hwang, "Cityflow: A city-scale benchmark for multi-target multi-camera vehicle tracking and re-identification," in *Proceedings of the IEEE/CVF Conference on Computer Vision and Pattern Recognition*, 2019, pp. 8797–8806.
- [43] V. Devyatkov, A. Alifimtsev, and A. Taranyan, "Multicamera human re-identification based on covariance descriptor," *Pattern Recognition and Image Analysis*, vol. 28, no. 2, pp. 232–242, 2018.
- [44] J. Guo, X. Zhu, C. Zhao, D. Cao, Z. Lei, and S. Z. Li, "Learning meta face recognition in unseen domains," in *Proceedings of the IEEE/CVF Conference on Computer Vision and Pattern Recognition*, 2020, pp. 6163–6172.
- [45] M. M. Kalayeh, E. Basaran, M. Gökmen, M. E. Kamasak, and M. Shah, "Human semantic parsing for person re-identification," in *Proceedings of the IEEE conference on computer vision and pattern recognition*, 2018, pp. 1062–1071.
- [46] W. J. Scheirer, A. de Rezende Rocha, A. Sapkota, and T. E. Boult, "Toward open set recognition," *IEEE transactions on pattern analysis and machine intelligence*, vol. 35, no. 7, pp. 1757–1772, 2012.
- [47] W. Bao, Q. Yu, and Y. Kong, "Evidential deep learning for open set action recognition," in *Proceedings of the IEEE/CVF International Conference on Computer Vision*, 2021, pp. 13 349–13 358.
- [48] Y. Gal and Z. Ghahramani, "Dropout as a bayesian approximation: Representing model uncertainty in deep learning," in *international conference on machine learning*. PMLR, 2016, pp. 1050–1059.
- [49] D. Molchanov, A. Ashukha, and D. Vetrov, "Variational dropout sparsifies deep neural networks," in *International Conference on Machine Learning*. PMLR, 2017, pp. 2498–2507.
- [50] Y. Gal, J. Hron, and A. Kendall, "Concrete dropout," *Advances in neural information processing systems*, vol. 30, 2017.
- [51] A. Amini, A. Soleimany, S. Karaman, and D. Rus, "Spatial uncertainty sampling for end-to-end control," *arXiv preprint arXiv:1805.04829*, 2018.
- [52] T. Pearce, M. Zaki, A. Brintrup, N. Anastassacos, and A. Neely, "Uncertainty in neural networks: Bayesian ensembling," *stat*, vol. 1050, p. 12, 2018.
- [53] B. Lakshminarayanan, A. Pritzel, and C. Blundell, "Simple and scalable predictive uncertainty estimation using deep ensembles," *Advances in neural information processing systems*, vol. 30, 2017.
- [54] C. Blundell, J. Cornebise, K. Kavukcuoglu, and D. Wierstra, "Weight uncertainty in neural network," in *International conference on machine learning*. PMLR, 2015, pp. 1613–1622.
- [55] J. M. Hernández-Lobato and R. Adams, "Probabilistic backpropagation for scalable learning of bayesian neural networks," in *International conference on machine learning*. PMLR, 2015, pp. 1861–1869.
- [56] A. Gelman, "Prior distributions for variance parameters in hierarchical models (comment on article by browne and draper)," *Bayesian analysis*, vol. 1, no. 3, pp. 515–534, 2006.
- [57] A. Gelman, A. Jakulin, M. G. Pittau, and Y.-S. Su, "A weakly informative default prior distribution for logistic and other regression models," *The annals of applied statistics*, vol. 2, no. 4, pp. 1360–1383, 2008.
- [58] A. Malinin and M. Gales, "Predictive uncertainty estimation via prior networks," *Advances in neural information processing systems*, vol. 31, 2018.
- [59] —, "Reverse kl-divergence training of prior networks: Improved uncertainty and adversarial robustness," *Advances in Neural Information Processing Systems*, vol. 32, 2019.
- [60] S. Kotz, N. Balakrishnan, and N. L. Johnson, *Continuous multivariate distributions, Volume 1: Models and applications*. John Wiley & Sons, 2004, vol. 1.
- [61] A. P. Dempster, *Classic works of the Dempster-Shafer theory of belief functions*, 2008.
- [62] S. Yu, D. Tan, and T. Tan, "A framework for evaluating the effect of view angle, clothing and carrying condition on gait recognition," in *ICPR*, vol. 4. IEEE, 2006, pp. 441–444.
- [63] Y. Lou, Y. Bai, J. Liu, S. Wang, and L.-Y. Duan, "Veri-wild: A large dataset and a new method for vehicle re-identification in the wild," in *Proceedings of the IEEE Conference on Computer Vision and Pattern Recognition*, 2019, pp. 3235–3243.
- [64] Y. Bai, J. Liu, Y. Lou, C. Wang, and L.-Y. Duan, "Disentangled feature learning network and a comprehensive benchmark for vehicle re-identification," in *In IEEE Transactions on Pattern Analysis and Machine Intelligence*, 2021.
- [65] F. Wan, Y. Wu, X. Qian, Y. Chen, and Y. Fu, "When person re-identification meets changing clothes," in *Proceedings of the IEEE/CVF Conference on Computer Vision and Pattern Recognition Workshops*, 2020, pp. 830–831.
- [66] H. Chao, Y. He, J. Zhang, and J. Feng, "Gaitset: Regarding gait as a set for cross-view gait recognition," in *Proceedings of the AAAI conference on artificial intelligence*, vol. 33, no. 01, 2019, pp. 8126–8133.
- [67] C. Fan, Y. Peng, C. Cao, X. Liu, S. Hou, J. Chi, Y. Huang, Q. Li, and Z. He, "Gaitpart: Temporal part-based model for gait recognition," in *Proceedings of the IEEE/CVF Conference on Computer Vision and Pattern Recognition*, 2020, pp. 14 225–14 233.
- [68] B. Lin, S. Zhang, and X. Yu, "Gait recognition via effective global-local feature representation and local temporal aggregation," in *Proceedings of the IEEE/CVF International Conference on Computer Vision*, 2021, pp. 14 648–14 656.
- [69] L. He, X. Liao, W. Liu, X. Liu, P. Cheng, and T. Mei, "Fastreid: A pytorch toolbox for general instance re-identification," *arXiv preprint arXiv:2006.02631*, 2020.
- [70] C. Fan, J. Liang, C. Shen, S. Hou, Y. Huang, and S. Yu, "Opengait: Revisiting gait recognition towards better practicality," in *Proceedings of the IEEE/CVF Conference on Computer Vision and Pattern Recognition*, 2023.
- [71] H. Luo, Y. Gu, X. Liao, S. Lai, and W. Jiang, "Bag of tricks and a strong baseline for deep person re-identification," in *Proceedings of the IEEE/CVF conference on computer vision and pattern recognition workshops*, 2019, pp. 0–0.
- [72] Z. Zhuang, L. Wei, L. Xie, T. Zhang, H. Zhang, H. Wu, H. Ai, and Q. Tian, "Rethinking the distribution gap of person re-identification with camera-based batch normalization," in *European Conference on Computer Vision*. Springer, 2020, pp. 140–157.
- [73] J. Yang, K. Zhou, Y. Li, and Z. Liu, "Generalized out-of-distribution detection: A survey," *arXiv preprint arXiv:2110.11334*, 2021.